# A Posteriori Error Estimates for the Weak Galerkin Finite Element Methods on Polytopal Meshes

Hengguang Li<sup>1</sup>, Lin Mu<sup>2,\*</sup> and Xiu Ye<sup>3</sup>

Received 7 March 2018; Accepted (in revised version) 16 July 2018

**Abstract.** In this paper, we present a simple a posteriori error estimate for the weak Galerkin (WG) finite element method for a model second order elliptic equation. This residual type estimator can be applied to general meshes such as hybrid, polytopal and those with hanging nodes. We prove the reliability and efficiency of the estimator. Extensive numerical tests demonstrate the effectiveness and flexibility of the mesh refinement guided by this error estimator.

AMS subject classifications: 65N15, 65N30, 35J50

**Key words**: Weak Galerkin, finite element methods, second-order elliptic problems, a posteriori error estimate, polytopal meshes.

#### 1 Introduction

Adaptive finite element methods [20] are widely used in modern computational science and engineering to obtain better accuracy with minimal effort. It can be achieved through adaptive mesh refinement that generates a mesh tailored in reducing computational errors at places of great need. Adaptive mesh refinement will be more local and effective for the finite element methods that allow general mesh [11, 13]. In recent years, many numerical schemes have been developed and analyzed on general polytopal mesh such as HDG method, mimetic finite difference method, virtual element method and hybrid high-order method [5,6,10,22].

A posteriori error analysis enables a measure of the reliability and efficiency of a particular numerical scheme employed for approximating the solution of partial differential

<sup>&</sup>lt;sup>1</sup> Department of Mathematics, Wayne State University, Detroit, MI 48202, USA.

<sup>&</sup>lt;sup>2</sup> Computer Science and Mathematics Division Oak Ridge National Laboratory, Oak Ridge, TN 37831, USA.

<sup>&</sup>lt;sup>3</sup> Department of Mathematics, University of Arkansas at Little Rock, Little Rock, AR 72204, USA.

<sup>\*</sup>Corresponding author. Email addresses: li@wayne.edu (H. Li), mull@ornl.gov (L. Mu), xxye@ualr.edu (X. Ye)

equations [1, 3, 24]. This result is a computable estimator that is an indicator of where the error is potentially large and specific elements need to be refined. A posteriori error analysis has been studied excessively for finite element methods with discontinuous approximation and we list few recent development of residual based a posteriori error estimates for the second order elliptic problems [2, 4, 7, 15, 16, 21, 29].

The weak Galerkin method is a natural extension of the standard Galerkin finite element method for discontinuous approximations. Its finite element formulation can be derived directly from the weak form of the corresponding partial differential equation where classical derivatives are substituted by weakly defined derivatives with a parameter-free stabilizer. Therefore, the weak Galerkin method has the flexibility of employing discontinuous elements and, at the same time, share the simple formulations of the continuous finite element methods. An important feature of the WG methods is allowing the use of general polytopal meshes [18,19,25,27]. The importance of such feature in adaptive finite element methods is well stated in [11,13].

An a posteriori error estimator has been developed and analyzed for the WG method in [9], in which only simplicial elements are considered. In this paper, we establish a new simple a posteriori error estimator for the weak Galerkin finite element approximation for using in the approximation of a second order elliptic equation. This error estimator has several unique features: 1) it can be applied on a general mesh such as polygonal/polyhedral mesh, hybrid mesh and mesh with hanging node. This feature is highly desirable in adaptive mesh refinement. 2) Our error estimator is simple containing only one term, a parameter free stabilizer, in addition to data oscillation. The common terms in error estimators such as area residual and flux jumps do not appear in our a posteriori estimator. Since the stabilizer has already been calculated in the process of obtaining the WG finite element approximation, there is no additional cost to compute the error estimator other than a high order data oscillation. 3) We obtain efficiency directly due to the simplicity of the error estimator. We prove the reliability of the a posteriori error estimator. Extensive numerical examples have been studied on different polygonal meshes to demonstrate the effectiveness and flexibility of the a posteriori error analysis.

For simplicity, we consider a simple model problem that seeks an unknown function u satisfying

$$-\Delta u = f, \quad \text{in } \Omega, \tag{1.1}$$

$$u = 0$$
, on  $\partial \Omega$ , (1.2)

where  $\Omega$  is a polytopal domain in  $\mathbb{R}^d$  (polygonal or polyhedral domain for d=2,3).

### 2 Weak Galerkin finite element schemes

Let  $\mathcal{T}_h$  be a partition of the domain  $\Omega$  consisting of polygons in two dimensions or polyhedra in three dimensions satisfying a set of conditions specified in [25].

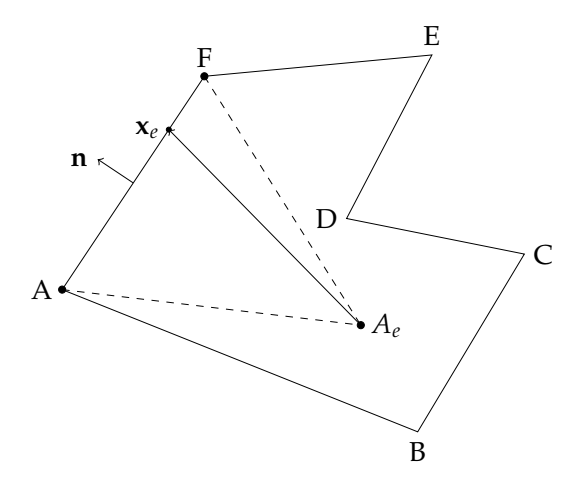


Figure 1: Depiction of a shape-regular polygonal element ABCDEFA.

Let  $\mathcal{T}_h$  be a partition of the domain  $\Omega$  consisting of elements which are closed and simply connected polygons in two dimensions or polyhedra in three dimensions; see Fig. 1. Let  $\mathcal{E}_h$  be the set of all edges or flat faces in  $\mathcal{T}_h$ , and  $\mathcal{E}_h^0 = \mathcal{E}_h \setminus \partial \Omega$  be the set of all interior edges or flat faces. Denote by  $h_T$  the diameter for every element  $T \in \mathcal{T}_h$  and  $h = \max_{T \in \mathcal{T}_h} h_T$  the mesh size for  $\mathcal{T}_h$ . We need some shape regularity assumptions for the partition  $\mathcal{T}_h$  described as below (cf. [25]).

**A1:** Assume that there exist two positive constants  $\varrho_v$  and  $\varrho_e$  such that for every element  $T \in \mathcal{T}_h$  we have

$$\varrho_v h_T^d \le |T|, \quad \varrho_e h_e^{d-1} \le |e| \tag{2.1}$$

for all edges or flat faces of *T*.

**A2:** Assume that there exists a positive constant  $\kappa$  such that for every element  $T \in \mathcal{T}_h$  we have

$$\kappa h_T \le h_e \tag{2.2}$$

for all edges or flat faces *e* of *T*.

**A3:** Assume that the mesh edges or faces are flat. We further assume that for every  $T \in \mathcal{T}_h$ , and for every edge/face  $e \in \partial T$ , there exists a pyramid  $P(e,T,A_e)$  contained in T such that its base is identical with e, its apex is  $A_e \in T$ , and its height is proportional to  $h_T$  with a proportionality constant  $\sigma_e$  bounded away from a fixed positive number  $\sigma^*$  from below. In other words, the height of the pyramid is given by  $\sigma_e h_T$  such that  $\sigma_e \geq \sigma^* > 0$ . The pyramid is also assumed to stand up above the base e in the sense that the angle between the vector  $\mathbf{x}_e - A_e$ , for any  $x_e \in e$ , and the outward normal direction of e is strictly acute by falling into an interval  $[0,\theta_0]$  with  $\theta_0 < \pi/2$ .

**A4:** Assume that each  $T \in \mathcal{T}_h$  has a circumscribed simplex S(T) that is shape regular and has a diameter  $h_{S(T)}$  proportional to the diameter of T; i.e.,  $h_{S(T)} \leq \gamma_* h_T$  with a constant  $\gamma_*$  independent of T. Furthermore, assume that each circumscribed simplex S(T) interests with only a fixed and small number of such simplices for all other elements  $T \in \mathcal{T}_h$ .

For a given integer  $k \ge 1$ , let  $V_h$  be the weak Galerkin finite element space associated with  $\mathcal{T}_h$  defined as follows

$$V_h = \{v = \{v_0, v_h\}: v_0|_T \in P_k(T), v_h|_e \in P_k(e), e \subset \partial T, T \in \mathcal{T}_h\}$$

and

$$V_h^0 = \{v \colon v \in V_h, v_b = 0 \text{ on } \partial\Omega\}.$$

We would like to emphasize that any function  $v \in V_h$  has a single value  $v_b$  on each edge  $e \in \mathcal{E}_h$ .

For any  $v = \{v_0, v_b\}$ , a weak gradient  $\nabla_w v \in [P_{k-1}(T)]^d$  is defined on T as the unique polynomial satisfying

$$(\nabla_w v, \tau)_T = -(v_0, \nabla \cdot \tau)_T + \langle v_b, \tau \cdot \mathbf{n} \rangle_{\partial T}, \quad \forall \tau \in [P_{k-1}(T)]^d. \tag{2.3}$$

Now we introduce some bilinear forms on  $V_h$  as follows:

$$\begin{split} s_T(v,w) &= h_T^{-1} \langle v_0 - v_b, w_0 - w_b \rangle_{\partial T}, \\ s(v,w) &= \sum_{T \in \mathcal{T}_h} s_T(v,w), \\ (\nabla_w v, \nabla_w w) &= \sum_{T \in \mathcal{T}_h} (\nabla_w v, \nabla_w w)_T. \end{split}$$

**Weak Galerkin Algorithm 1.** Find  $u_h \in V_h^0$  satisfying the following equation:

$$(\nabla_w u_h, \nabla_w v) + s(u_h, v) = (f, v), \quad \forall \ v \in V_h^0.$$

$$(2.4)$$

Define a discrete  $H^1$  equivalent norm,

$$|||v|||^2 = (\nabla_w v, \nabla_w v) + s(v, v).$$
 (2.5)

The following theorem can be found in [17].

**Theorem 2.1.** Let  $u_h \in V_h$  be the weak Galerkin finite element solution of the problem (1.1)-(1.2) arising from (2.4). Assume the exact solution  $u \in H^{k+1}(\Omega)$ , then, there exists a constant C such that

$$|||u - u_h||| \le Ch^k ||u||_{k+1},$$
 (2.6)

$$||u - u_h|| \le Ch^{k+1} ||u||_{k+1}. \tag{2.7}$$

## 3 A posteriori error estimator for the WG method

For simplicity of notation, results shall be presented in two dimensions noting that the results can be extended to three-dimensional space. First, define a differential operator for a scalar function  $\boldsymbol{v}$ 

$$\nabla \times v = \left(-\frac{\partial v}{\partial x_2}, \frac{\partial v}{\partial x_1}\right).$$

Let  $f_h$  be the  $L^2$  projection of f to  $V_h$ . Then we introduce a local estimator as follows

$$\eta_T^2 = s_T(u_h, u_h) + osc^2(f, T),$$
(3.1)

where osc(f,T) is a high order local data oscillation if f is smooth enough defined by

$$osc^{2}(f,T) = h_{T}^{2} ||f - f_{h}||_{T}^{2}$$

Define a global error estimator and data oscillation as

$$\eta^2 = \sum_{T \in \mathcal{T}_h} \eta_T^2,$$

$$osc(f, \mathcal{T}_h)^2 = \sum_{T \in \mathcal{T}_h} osc(f, T)^2.$$

Let *T* be an element with *e* as an edge. It is well known that there exists a constant *C* such that for any function  $g \in H^1(T)$ 

$$||g||_{e}^{2} \le C\left(h_{T}^{-1}||g||_{T}^{2} + h_{T}||\nabla g||_{T}^{2}\right). \tag{3.2}$$

For each element  $T \in \mathcal{T}_h$ , denote by  $Q_0$  the  $L^2$  projection from  $L^2(T)$  to  $P_k(T)$  and by  $Q_b$  the  $L^2$  projection from  $L^2(e)$  to  $P_k(e)$ . Denote by  $Q_h$  the  $L^2$  projection from  $[L^2(T)]^2$  to a local weak gradient space  $[P_{k-1}(T)]^2$ . Define  $Q_h u = \{Q_0 u, Q_h u\} \in V_h$ .

**Lemma 3.1.** On each element  $T \in \mathcal{T}_h$ , we have the following commutative property for  $\phi \in H^1(T)$ ,

$$\nabla_{w}(Q_{h}\phi) = Q_{h}(\nabla\phi), \tag{3.3}$$

$$\nabla_{w}\phi = \mathbb{Q}_{h}(\nabla\phi). \tag{3.4}$$

*Proof.* Using (2.3), the integration by parts and the definition of  $\mathbb{Q}_h$ , we have that for any  $\tau \in [P_{k-1}(T)]^2$ 

$$(\nabla_w \phi, \tau)_T = -(\phi, \nabla \cdot \tau)_T + \langle \phi, \tau \cdot \mathbf{n} \rangle_{\partial T} = (\nabla \phi, \tau)_T = (\mathbb{Q}_h(\nabla \phi), \tau)_T$$

which implies (3.4). The proof of the identity (3.3) can be found in [17].

We define  $H(\text{div};\Omega)$  as the set of vector-valued functions on  $\Omega$  which, together with their divergence, are square integrable; i.e.,

$$H(\operatorname{div};\Omega) = \left\{ \mathbf{v} : \mathbf{v} \in [L^2(\Omega)]^d, \nabla \cdot \mathbf{v} \in L^2(\Omega) \right\}.$$

**Lemma 3.2.** For  $u_h \in V_h^0$  and  $\phi \in H^1(\Omega)$ , we have

$$(\nabla u - \nabla_w u_h, \nabla \times \phi) \le C s^{1/2} (u_h, u_h) \|\nabla \times \phi\|. \tag{3.5}$$

*Proof.* Since  $\nabla \times \phi \in H(\text{div}, \Omega)$  and  $u \in H_0^1(\Omega)$ , we have

$$(\nabla u - \nabla_w u_h, \nabla \times \phi) = (\nabla u, \nabla \times \phi) - (\nabla_w u_h, \nabla \times \phi) = -(\nabla_w u_h, \nabla \times \phi). \tag{3.6}$$

First, assume  $s_T(u_h, u_h) \neq 0$ . For  $e \subset \partial T$ , it is obvious that  $u_b \in H^{1/2}(e)$ . Since  $C_0^{\infty}(e)$  is dense in  $H^{1/2}(e)$  (see Theorem 1.4.2.4 in [14]), there exists  $u_b^e \in C_0^{\infty}(e)$  for each e such that  $u_b^e = 0$  on  $\partial \Omega$  and

$$h_T^{-1} \| u_b - u_b^e \|_{H^{1/2}(e)}^2 \le Cs_T(u_h, u_h).$$
 (3.7)

Define  $\widetilde{u}_b$  on  $\partial T$  such that  $\widetilde{u}_b = u_b^e$  on  $e \subset \partial T$ . Then we have  $\widetilde{u}_b \in H^{1/2}(\partial T)$ . If  $s_T(u_h, u_h) = 0$ , let  $\widetilde{u}_b = u_b \in H^{1/2}(\partial T)$ .

It follows from (2.3),  $u_h \in V_h^0$  and the integration by parts,

$$\begin{split} \sum_{T \in \mathcal{T}_h} (\nabla_w u_h, \nabla \times \phi)_T &= \sum_{T \in \mathcal{T}_h} (\nabla_w u_h, \mathbb{Q}_h \nabla \times \phi)_T \\ &= \sum_{T \in \mathcal{T}_h} (-(u_0, \nabla \cdot (\mathbb{Q}_h \nabla \times \phi))_T + \langle u_b, \mathbb{Q}_h \nabla \times \phi \cdot \mathbf{n} \rangle_{\partial T}) \\ &= \sum_{T \in \mathcal{T}_h} ((\nabla u_0, \mathbb{Q}_h \nabla \times \phi)_T - \langle u_0, \mathbb{Q}_h \nabla \times \phi \cdot \mathbf{n} \rangle_{\partial T} + \langle u_b, \mathbb{Q}_h \nabla \times \phi \cdot \mathbf{n} \rangle_{\partial T}) \\ &= \sum_{T \in \mathcal{T}_h} ((\nabla u_0, \nabla \times \phi)_T - \langle u_0, \mathbb{Q}_h \nabla \times \phi \cdot \mathbf{n} \rangle_{\partial T} + \langle u_b, \mathbb{Q}_h \nabla \times \phi \cdot \mathbf{n} \rangle_{\partial T}) \\ &= \sum_{T \in \mathcal{T}_h} (-\langle u_0, (\mathbb{Q}_h \nabla \times \phi - \nabla \times \phi) \cdot \mathbf{n} \rangle_{\partial T} + \langle u_b, \mathbb{Q}_h \nabla \times \phi \cdot \mathbf{n} \rangle_{\partial T}) \\ &= \sum_{T \in \mathcal{T}_h} (-\langle u_0 - \widetilde{u}_b, (\mathbb{Q}_h \nabla \times \phi - \nabla \times \phi) \cdot \mathbf{n} \rangle_{\partial T} + \langle u_b - \widetilde{u}_b, \mathbb{Q}_h \nabla \times \phi \cdot \mathbf{n} \rangle_{\partial T}) \\ &= \sum_{T \in \mathcal{T}_h} (\langle u_0 - \widetilde{u}_b, \nabla \times \phi \cdot \mathbf{n} \rangle_{\partial T} - \langle u_0 - \widetilde{u}_b, \mathbb{Q}_h \nabla \times \phi \cdot \mathbf{n} \rangle_{\partial T} + \langle u_b - \widetilde{u}_b, \mathbb{Q}_h \nabla \times \phi \cdot \mathbf{n} \rangle_{\partial T}) \\ &= \sum_{T \in \mathcal{T}_h} (\langle u_0 - \widetilde{u}_b, \nabla \times \phi \cdot \mathbf{n} \rangle_{\partial T} - \langle u_0 - \widetilde{u}_b, \mathbb{Q}_h \nabla \times \phi \cdot \mathbf{n} \rangle_{\partial T} + \langle u_b - \widetilde{u}_b, \mathbb{Q}_h \nabla \times \phi \cdot \mathbf{n} \rangle_{\partial T}) \end{split}$$

We will bound the three terms on the right hand side of the equation above one by one. Using the Cauchy-Schwarz inequality, (3.7), the inverse inequality and the fact  $\nabla \cdot \nabla \times \phi = 0$ , we arrive at

$$\begin{split} \langle u_{0} - \widetilde{u}_{b}, \nabla \times \phi \cdot \mathbf{n} \rangle_{\partial T} &\leq \|u_{0} - \widetilde{u}_{b}\|_{H^{1/2}(\partial T)} \|\nabla \times \phi \cdot \mathbf{n}\|_{H^{-1/2}(\partial T)} \\ &\leq C \left( \sum_{e \subset \partial T} \left( \|u_{0} - u_{b}\|_{H^{1/2}(e)}^{2} + \|u_{b} - u_{b}^{e}\|_{H^{1/2}(e)}^{2} \right) \right)^{1/2} \|\nabla \times \phi\|_{H(\operatorname{div}, T)} \\ &\leq C \left( \sum_{e \subset \partial T} \left( h_{T}^{-1} \|u_{0} - u_{b}\|_{e}^{2} + \|u_{b} - u_{b}^{e}\|_{H^{1/2}(e)}^{2} \right) \right)^{1/2} \|\nabla \times \phi\|_{H(\operatorname{div}, T)} \\ &\leq C s_{T}^{-1/2} (u_{h}, u_{h}) \|\nabla \times \phi\|_{T}. \end{split}$$

The Cauchy-Schwarz inequality, the trace inequality, the inverse inequality and (3.7) imply

$$\begin{aligned} \langle u_0 - \widetilde{u}_b, \mathbf{Q}_h \nabla \times \phi \cdot \mathbf{n} \rangle_{\partial T} &\leq \|u_0 - \widetilde{u}_b\|_{\partial T} \|\mathbf{Q}_h \nabla \times \phi \cdot \mathbf{n}\|_{\partial T} \\ &\leq C \left( \sum_{e \subset \partial T} h_T^{-1} \Big( \|u_0 - u_b\|_e^2 + \|u_b - u_b^e\|_e^2 \Big) \right)^{1/2} \|\nabla \times \phi\|_T \\ &\leq C s_T^{1/2} (u_h, u_h) \|\nabla \times \phi\|_T. \end{aligned}$$

Similarly, we can have

$$\langle u_b - \widetilde{u}_b, \mathbb{Q}_h \nabla \times \phi \cdot \mathbf{n} \rangle_{\partial T} \leq C s_T^{1/2}(u_h, u_h) \| \nabla \times \phi \|_T.$$

Combining all the estimates above with (3.6), we have completed the proof.

**Theorem 3.1.** Let  $u_h \in V_h^0$  and  $u \in H_0^1(\Omega)$  be the solutions of (2.4) and (1.1)-(1.2) respectively. Then there exists a positive constant C such that,

$$|||u - u_h||^2 \le C\eta^2. \tag{3.8}$$

*Proof.* We shall apply Helmholtz decomposition first. It is well known [12] that for  $\nabla_w u - \nabla_w u_h \in [L^2(\Omega)]^2$ , there exist  $\psi \in H^1_0(\Omega)$  and  $\phi \in H^1(\Omega)$  such that

$$\nabla_w u - \nabla_w u_h = \nabla \psi + \nabla \times \phi \tag{3.9}$$

and that

$$\|\nabla_w u - \nabla_w u_h\|^2 = \|\nabla \psi\|^2 + \|\nabla \times \phi\|^2. \tag{3.10}$$

It follows from (3.9) and (3.4),

$$\|\nabla_{w}u - \nabla_{w}u_{h}\|^{2} = (\nabla_{w}u - \nabla_{w}u_{h}, \nabla_{w}u - \nabla_{w}u_{h})$$

$$= (\nabla u - \nabla_{w}u_{h}, \nabla_{w}u - \nabla_{w}u_{h})$$

$$= (\nabla u - \nabla_{w}u_{h}, \nabla\psi) + (\nabla u - \nabla_{w}u_{h}, \nabla \times \phi).$$
(3.11)

Using (3.3) and (3.10), we have

$$(\nabla u - \nabla_w u_h, \nabla \psi) = (\nabla u, \nabla \psi) - (\nabla_w u_h, \nabla \psi)$$

$$= (f, \psi) - (\nabla_w u_h, \nabla_w Q_h \psi)$$

$$= (f, \psi) - (f, Q_0 \psi) + s(u_h, Q_h \psi)$$

$$= (f - f_h, \psi - Q_0 \psi) + \sum_{T \in \mathcal{T}_h} h^{-1} \langle u_0 - u_h, Q_0 \psi - Q_h \psi \rangle_{\partial T}$$

$$\leq (osc(f, \mathcal{T}_h) + s^{1/2}(u_h, u_h)) \| \nabla \psi \|$$

$$\leq (osc(f, \mathcal{T}_h) + s^{1/2}(u_h, u_h)) \| \nabla_w u - \nabla_w u_h \|. \tag{3.12}$$

It follows from (3.5),

$$(\nabla u - \nabla_w u_h, \nabla \times \phi) \le C s^{1/2} (u_h, u_h) \|\nabla \times \phi\|. \tag{3.13}$$

Using (3.10), (3.11), (3.12) and (3.13), we have

$$\|\nabla_w u - \nabla_w u_h\|^2 \le C\eta^2$$
.

Next we easily have

$$s(u-u_h, u-u_h) = s(u_h, u_h) \le \eta^2$$
.

Thus we have proved the theorem.

Define

$$|||v|||_T^2 = (\nabla_w v, \nabla_w v)_T + s_T(v, v).$$
 (3.14)

Then we can obtain the following local lower bound automatically.

**Lemma 3.3.** *The local estimator*  $\eta_T$  *is defined in* (3.1). *Then* 

$$\eta_T^2 \le ||u - u_h||_T^2 + osc^2(f, T).$$
 (3.15)

Proof. It follows from (3.1) and (3.14) that

$$\eta_T^2 = s_T(u_h, u_h) + osc^2(f, T) 
\leq (\nabla_w u_h, \nabla_w u_h)_T + s_T(u_h, u_h) + osc^2(f, T) 
= |||u - u_h|||_T^2 + osc^2(f, T).$$

We have completed the proof.

# 4 Numerical examples

In this section, we shall validate the proposed algorithm for several tests. First, we shall explore the convergence properties of errors measured in  $\|\cdot\|$ -norm (denoted by  $H^1$ -error in tables and  $H^1$ -err in figures) and the estimator  $\eta$ . The effectivity of the estimator is defined as follows,

$$Eff-index = \frac{\eta}{\|Q_h u - u_h\|}.$$
 (4.1)

**Example 4.1.** Let  $\Omega = (0,1)^2$ , and the function f is taken to satisfy the Eqs. (1.1)-(1.2) such that the exact solution can be described as

$$u = \sin(\pi x)\sin(\pi y)$$
.

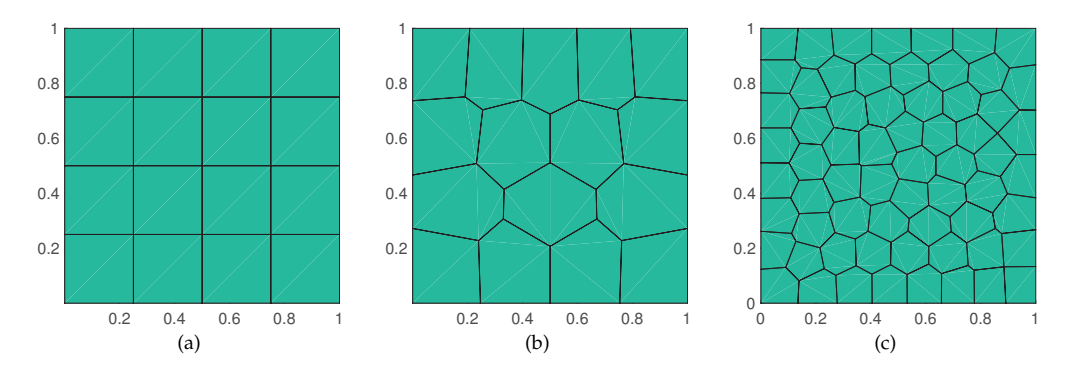


Figure 2: Example 4.1: (a) rectangular mesh of level 1; (b) polygonal mesh of level 1; (c) polygonal mesh of level 2.

Weak Galerkin algorithm (2.4) is applied on two different meshes, shown in Fig. 2 (a) and (b). Fig. 2 (a) is the uniform rectangular mesh, which has mesh size  $h = 1/N_x$ .

The numerical approximation, on uniform rectangular meshes, starts on the initial mesh with  $N_x = 4$ , and then performs on a sequence of uniform rectangular meshes.

Table 1: Example 4.1: Rates of convergence of the discrete  $H^1$ -error and estimator  $\eta$  for the weak Galerkin finite element solution on rectangular meshes 2 (a).

$N_{\chi}$	$H^1$ -error	order	Estimator $\eta$	order	Eff-index			
	p=1							
4	1.0033E+00		1.2626E+00		1.2584			
8	5.1101E-01	0.97	6.3875E-01	0.98	1.2500			
16	2.5664E-01	0.99	3.2059E-01	0.99	1.2492			
32	1.2846E-01	1.00	1.6046E-01	1.00	1.2491			
64	6.4249E-02	1.00	8.0248E-02	1.00	1.2490			
128	3.2127E-02	1.00	4.0127E-02	1.00	1.2490			
	p=2							
4	2.5700E-01		2.9862E-01		1.1619			
8	6.7403E-02	1.93	7.9155E-02	1.92	1.1744			
16	1.7086E-02	1.98	2.0172E-02	1.97	1.1806			
32	4.2869E-03	1.99	5.0691E-03	1.99	1.1825			
64	1.0727E-03	2.00	1.2689E-03	2.00	1.1829			
128	2.6823E-04	2.00	3.1734E-04	2.00	1.1831			
	p=3							
4	4.0007E-02		4.4904E-02		1.1224			
8	5.1991E-03	2.94	5.8856E-03	2.93	1.1320			
16	6.5722E-04	2.98	7.4707E-04	2.98	1.1367			
32	8.2394E-05	3.00	9.3772E-05	2.99	1.1381			
64	1.0307E-05	3.00	1.1743E-05	3.00	1.1393			
128	1.2886E-06	3.00	1.4607E-06	3.01	1.1336			

Mesh Level	H <sup>1</sup> -error	order	Estimator $\eta$	order	Eff-index		
	p=1						
Level 1	8.7105E-01		1.1610E+00		1.3329		
Level 2	4.3885E-01	0.99	5.9583E-01	0.96	1.3577		
Level 3	2.2329E-01	0.97	3.0700E-01	0.96	1.3749		
Level 4	1.1593E-01	0.95	1.5776E-01	0.96	1.3608		
Level 5	5.7931E-02	1.00	7.9188E-02	0.99	1.3669		
Level 6	2.9135E-02	0.99	3.9851E-02	0.99	1.3678		
	p=2						
Level 1	2.1981E-01		2.6401E-01		1.2011		
Level 2	5.3164E-02	2.05	6.4738E-02	2.03	1.2177		
Level 3	1.2972E-02	2.04	1.5834E-02	2.03	1.2206		
Level 4	3.2348E-03	2.00	3.9606E-03	2.00	1.2244		
Level 5	8.0119E-04	2.01	9.7720E-04	2.02	1.2197		
Level 6	1.9711E-04	2.02	2.4105E-04	2.02	1.2229		
	p=3						
Level 1	3.4170E-02		3.9341E-02		1.1513		
Level 2	3.8366E-03	3.15	4.3736E-03	3.17	1.1400		
Level 3	4.7189E-04	3.02	5.4134E-04	3.01	1.1472		
Level 4	5.7227E-05	3.04	6.5638E-05	3.04	1.1470		
Level 5	6.7425E-06	3.09	7.7012E-06	3.09	1.1422		
Level 6	8.4961E-07	2.99	9.7080E-07	2.99	1.1426		

Table 2: Example 4.1: Rates of convergence of the discrete  $H^1$ -error and estimator  $\eta$  for the weak Galerkin finite element solution on polygonal meshes 2 (b).

The error profiles and convergence history for weak Galerkin finite element with weak Galerkin element of degree p=1,2,3 are reported in Table 1. It is observed that the convergence rates for  $H^1$ -error and  $\eta$  are at order  $\mathcal{O}(h^p)$  and the effectivity becomes a constant with decreasing mesh size  $h=1/N_x$ . All of these observations confirm the previous theoretical conclusions.

Besides the uniform rectangular mesh, a numerical simulation has also been performed on polytopal meshes. A sequence of the polytopal meshes are generated by mesh generator POLYMESHER [23]. The first level and second level of meshes are shown as Fig. 2 (b) and (c) respectively. Table 2 reports error profiles and convergence rate, which again confirms the theory.

The following adaptivity test shall use a typical adaptive algorithm:

Solve 
$$\rightarrow$$
 Estimate  $\rightarrow$  Mark  $\rightarrow$  Refine.

In our numerical experiments, the following adaptive steps shall be performed:

A. We solve weak Galerkin numerical solution  $u_h^{(i)}$  on a given polygonal mesh  $\mathcal{T}_h^{(i)}$ ;

- B. Estimate the a posteriori error estimator  $\eta_T^{(i)}$  and  $\eta^{(i)}$ ;
- C. Mark the elements require refinement guided by the calculated error estimator  $\eta_T^{(i)}$ ;
- D. Refine the marked elements, and then derive the updated polygonal mesh  $\mathcal{T}_h^{(i+1)}$ ;
- E. Repeat Steps A-D until the maximum iteration number is reached or a stopping criteria is satisfied.

Here, the Dörfler/bulk marking method  $(\eta_T^{(i)} \geq \gamma \eta_{\max}^{(i)}, \text{ with } \eta_{\max}^{(i)} = \max_{T \in \mathcal{T}_h^{(i)}} \eta_T^{(i)})$  with parameter  $\gamma = 0.2$  will be used in the mark procedure. All the numerical tests are perform on MATLAB and backslash (\) from MATLAB has been used for linear solver.

We follow the similar idea in the reference [8] to refine polygonal element. For a marked polygonal element T, the refinement is obtained by connecting the midpoint of each element face to its barycentre, which is shown in Fig. 3. By this refinement approach, hanging nodes maybe introduced on edges. It will be demonstrated that we can treat elements with hanging node as multi-edge polygons and then perform weak Galerkin finite element simulation. The flexibility of imposing arbitrary numbers of hanging node can avoid local post-processing (such as refinement of neighbor elements), and thus provide more flexibility for developing adaptive mesh generation methods.

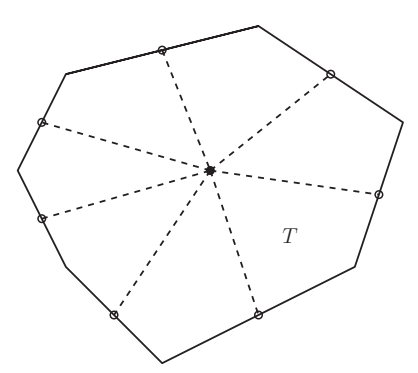


Figure 3: Illustration of the refinement strategy for polygonal element T.

**Example 4.2.** Let  $\Omega = (0,1)^2$ , and the exact solution is chosen as

$$u = \exp(-1000(x - 0.5)^2 - 1000(y - 0.5)^2). \tag{4.2}$$

This test contains an exponential peak located in the interior of the domain at (0.5,0.5), shown in Fig. 4(a).

We start with initial mesh as shown in Fig. 4(b) for weak Galerkin approximation of weak Galerkin element of degree p = 1,2,3. The final refinements are plotted in Fig. 5 for different weak Galerkin finite elements and stopping criteria. It demonstrates that our

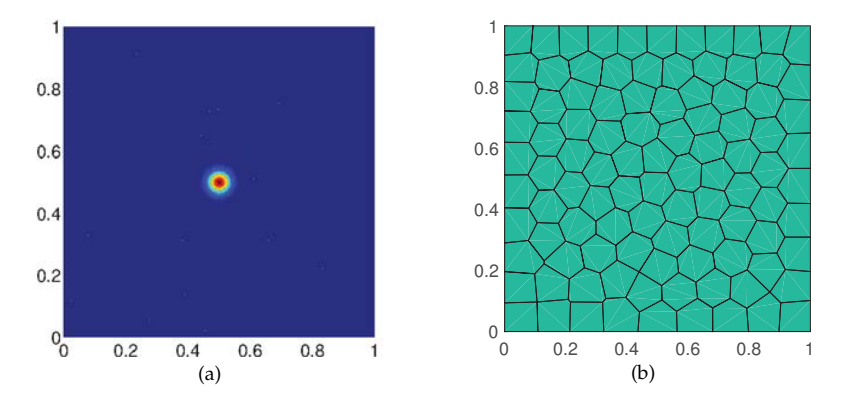


Figure 4: Example 4.2: (a) Solution of the problem; (b) Mesh Level 1.

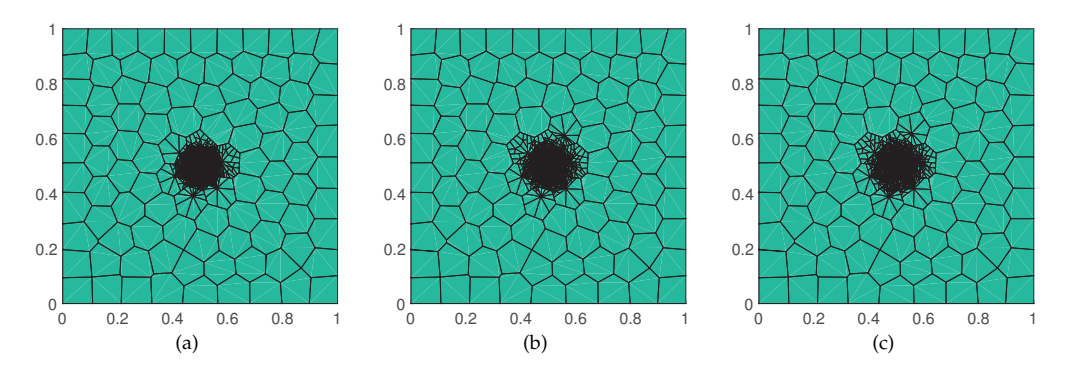


Figure 5: Example 4.2: (a) Final refined mesh for weak Galerkin element of  $p\!=\!1$  for stopping criteria  $\eta\!<\!1e\!-\!1$ ; (b) Final refined mesh for weak Galerkin element of  $p\!=\!2$  for stopping criteria  $\eta\!<\!1e\!-\!2$ ; (c) Final refined mesh for weak Galerkin element of  $p\!=\!3$  for stopping criteria  $\eta\!<\!1e\!-\!3$ .

a posteriori error estimator  $\eta$  can locate the position of the peak. The error profiles and convergence results are plotted in Fig. 6. It can be seen that the rate of convergence is of the theoretical optimal rate as Dofs<sup>-p/2</sup>.

**Example 4.3.** In this test, a adaptive refinement algorithms shall be performed for the problem with steep wave front. Let domain  $\Omega = (0,1)^2$  and exact solution is as follows,

$$u = \arctan(\alpha(r-r_0)),$$

with  $r = \sqrt{(x-x_0)^2 + (y-y_0)^2}$  and  $\alpha = 1000$ ,  $x_0 = -0.05$ ,  $y_0 = -0.05$ , and  $r_0 = 0.7$ . In this test, the circular wave front is given by an arctangent. For the arctangent, there is a mild singularity at the center of the circle (-0.05, -0.05), which locates at the outside the domain. Thus, we can exam only investigate the performance on the wave front, shown as Fig. 7.

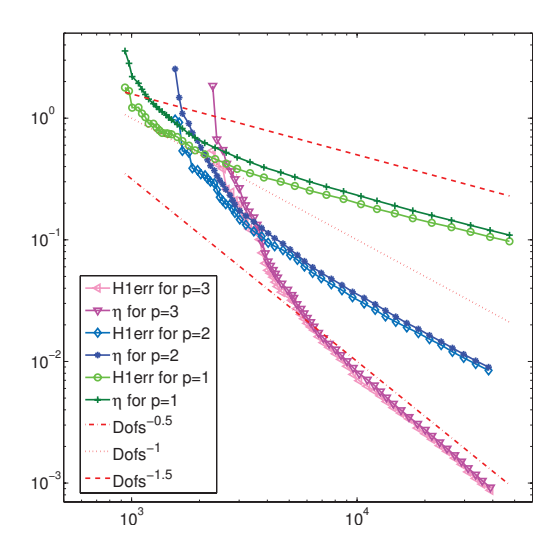


Figure 6: Example 4.2: Convergence of  $H^1$ -error and error estimator  $\eta$ .

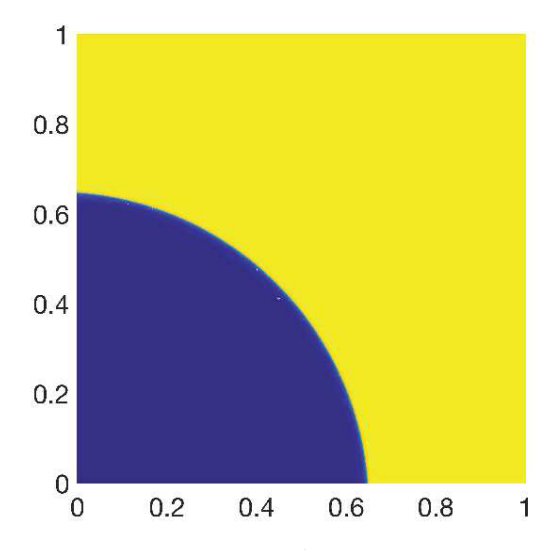


Figure 7: Example 4.3: Solution of the problem.

The weak Galerkin finite elements with p=1,2,3 are performed on the polygonal mesh (Fig. 9 (a)) and randomised quadrilateral mesh (Fig. 9 (b)). The error profiles and convergence results are plotted in Fig. 8. The theoretical optimal rates (Dofs<sup>-p/2</sup>) are achieved for all the tests on polygonal mesh and randomised quadrilateral mesh. Moreover, the final refined meshes are plotted in Fig. 9, which shows that the refinement guided by the proposed error estimator can capture the front wave along a quarter of the circle centered at  $x_0 = -0.05$ ,  $y_0 = -0.05$ .

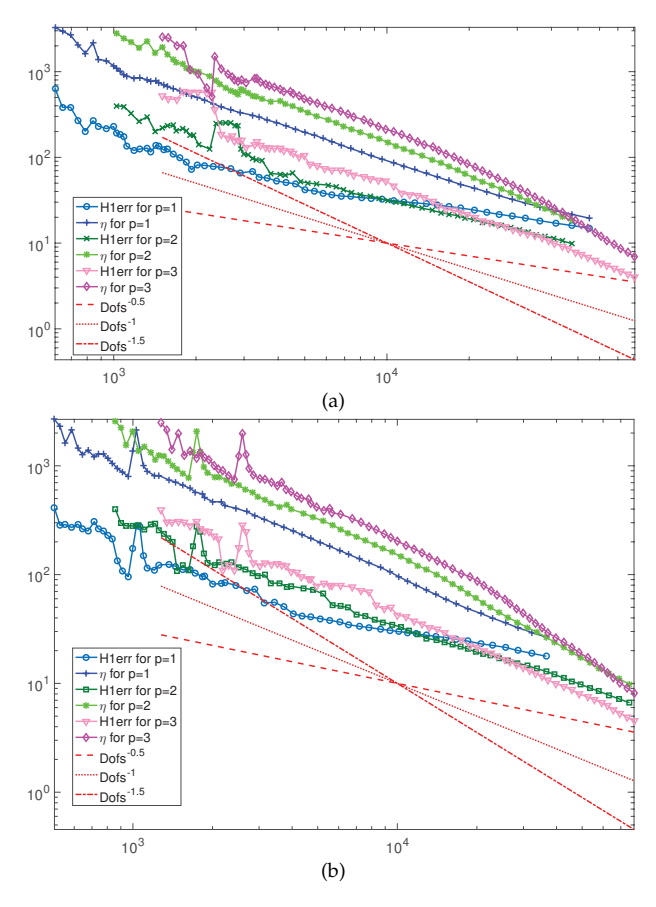


Figure 8: Example 4.3: (a) Convergence results for polygonal initial mesh; (b) Convergence results for randomised quadrilateral initial mesh.

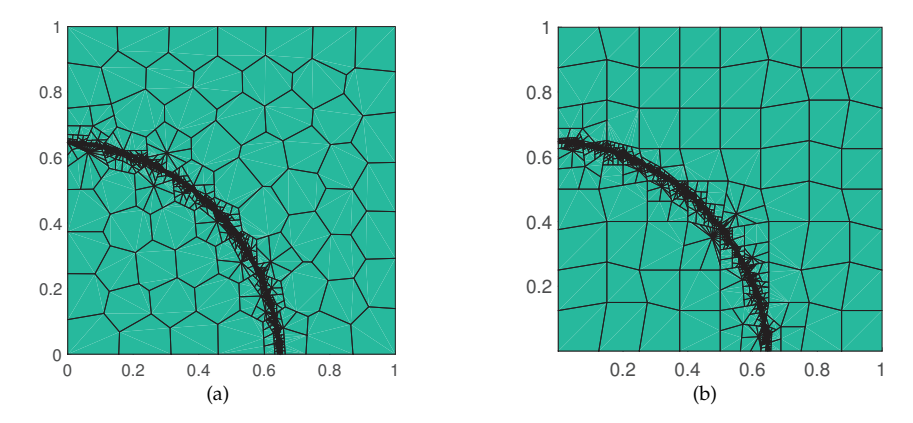


Figure 9: Example 4.3: (a) Final refined mesh on the polygonal mesh; (b) Final refined mesh on the randomised quadrilateral mesh.

**Example 4.4.** In this example, let  $\Omega = (0,1)^2$ , and we shall test the Poisson problem with following exact solution:

$$u = x(1-x)y(1-y)r^{-2+t},$$
 (4.3)

where *t* is a parameter. It is known that the solution  $u \in H^{1+t-\epsilon}(\Omega)$  for  $\epsilon > 0$ .

First test is performed for t = 1/2 on the uniform refinement of rectangular mesh. Numerical results are reported in Table 3. The solution for t = 1/2 is plotted in Fig. 10 (a). It can be observed that for polynomials with degree p = 1,2,3, the error is converging at order  $\mathcal{O}(h^{0.5})$  because of the singularity at origin.

In order to solve this singular problem more efficiently, the adaptive strategy of proposed a posteriori error estimator is used to locate the singularity and refine the local mesh accordingly. Weak Galerkin finite element method shall be applied on the initial rectangular mesh for t = 0.5 and initial polygonal mesh for t = 0.1. Fig. 10 (b) and Fig. 12 plot the refinement of rectangular initial mesh. Convergence results are plotted in Fig. 11 and Fig. 13, which confirms our theoretical conclusions.

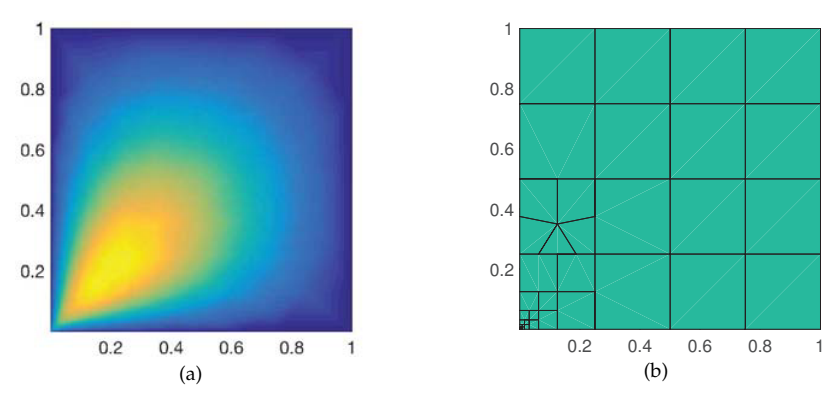


Figure 10: Example 4.4 with t = 0.5: (a) Solution; (b) Final refined mesh for  $\eta < 1e - 2$ .

**Example 4.5.** We shall test L-shape problem. The L-shaped domain is contained within  $(-1,1)^2\setminus(0,1)\times(-1,0)$  and exhibiting low regularity at the reentrant corner, located at the origin. This problem has the solution

$$u(x,y) = r^{2/3}\sin(2\theta/3),$$
 (4.4)

where  $(r,\theta)$  are the usual polar coordinates.

For the numerical test, we start with initial polygonal mesh and rectangular mesh, and the final refined meshes for stopping criteria  $\eta < 1\mathrm{e} - 3$  with polynomial degree p = 1 are plotted in Fig. 14. It can be seen that the refinement is around the singularity (origin), and thus validate our conclusions.

**Example 4.6.** Let domain  $\Omega = (0,1)^2$  with a sharp layer in the interior of the domain and solution is chosen as,

$$u(x,y) = 16x(1-x)y(1-y)\arctan(25x-100y+50).$$
 (4.5)

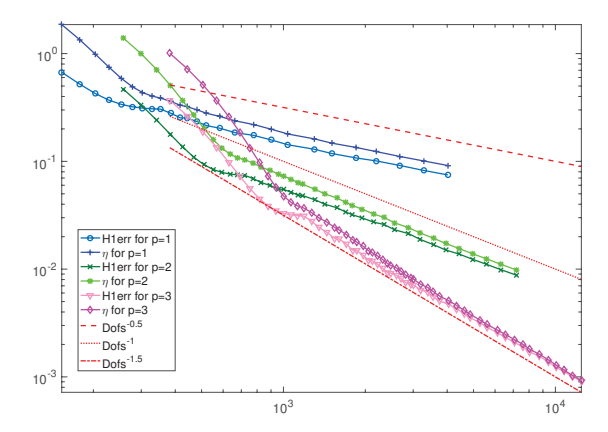


Figure 11: Example 4.4 with t = 0.5: Convergence results for rectangular initial mesh.

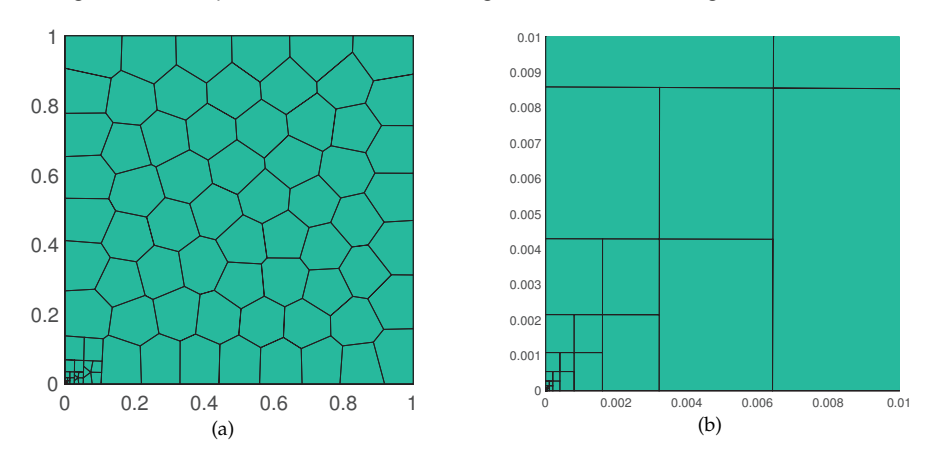


Figure 12: Example 4.4 with  $t=1\mathrm{e}-1$ : (a) Final Refinement of polygonal mesh for  $\eta < 1\mathrm{e}-2$ ; (b) Zoom in at  $(0,0.01)^2$ .

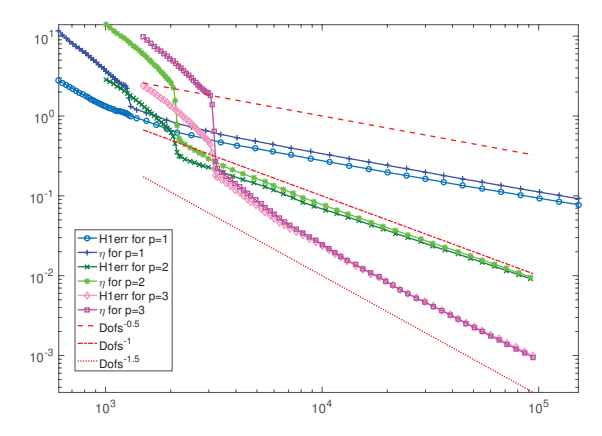
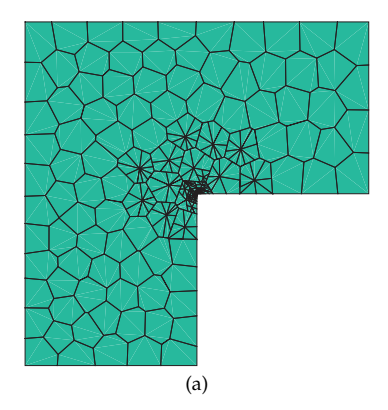


Figure 13: Example 4.4 with t = 1e - 1: Convergence results for polygonal initial mesh.

Table 3: Example 4.4: Rates of convergence of the discrete  $H^1$ -error and estimator  $\eta$  for the weak Galerkin finite element solution on uniform rectangular meshes for t=1/2.

$N_x$	$H^1$ -error	order	Estimator $\eta$	order	Eff-index			
	p=1							
4	8.9407E-01		2.5692E+00		2.8736			
8	6.5084E-01	0.46	1.8473E+00	0.48	2.8383			
16	4.6768E-01	0.48	1.3189E+00	0.49	2.8201			
32	3.3372E-01	0.49	9.3753E-01	0.49	2.8093			
64	2.3720E-01	0.49	6.6482E-01	0.50	2.8028			
128	1.6822E-01	0.50	4.7080E-01	0.50	2.7987			
	p=2							
4	6.6023E-01		1.9433E+00		2.9434			
8	4.6455E-01	0.51	1.3923E+00	0.48	2.9971			
16	3.2796E-01	0.50	9.9158E-01	0.49	3.0235			
32	2.3179E-01	0.50	7.0380E-01	0.49	3.0364			
64	1.6388E-01	0.50	4.9863E-01	0.50	3.0427			
128	1.1588E-01	0.50	3.5293E-01	0.50	3.0457			
	p=3							
4	5.1654E-01		1.3947E+00		2.7001			
8	3.6835E-01	0.49	1.0067E+00	0.47	2.7330			
16	2.6189E-01	0.49	7.1969E-01	0.48	2.7481			
32	1.8575E-01	0.50	5.1180E-01	0.49	2.7553			
64	1.3156E-01	0.50	3.6294E-01	0.50	2.7587			
128	9.3102E-02	0.50	2.5701E-01	0.50	2.7605			



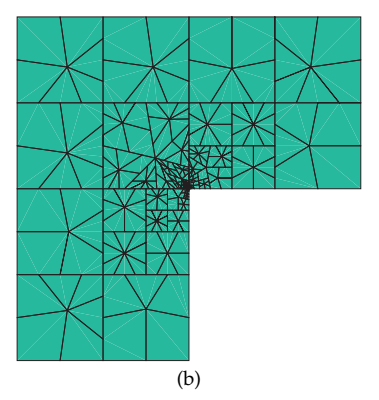


Figure 14: Example 4.5 for p=1: (a) Final Refinement of polygonal initial mesh for  $\eta < 1\mathrm{e} - 3$ ; (b) Final Refinement of rectangular initial mesh for  $\eta < 1\mathrm{e} - 3$ .

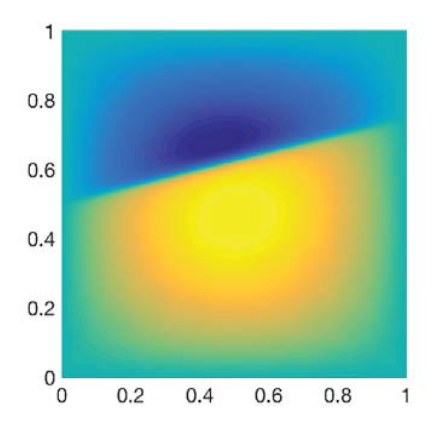


Figure 15: Example 4.6: Solution.

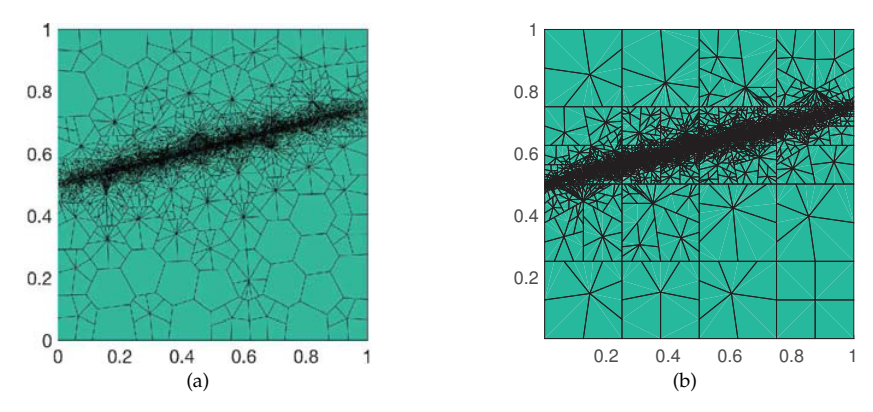


Figure 16: Example 4.6: (a) Final refined mesh of initial polygonal mesh for  $\eta < 1e-2$ ; (b) Final refined mesh of initial rectangular mesh for  $\eta < 1e-2$ .

The performance of the error and estimator through adaptive procedure is shown in Fig. 17 for initial polygonal mesh. Again the error convergences with the theoretical optimal rate at Dofs $^{-p/2}$ . Also the final refinement with stopping criteria  $\eta < 1\mathrm{e} - 2$  is shown in Fig. 16, which shows that the proposed error estimator can capture the sharp interior layer.

**Example 4.7.** In this test, we take L-shape domain  $\Omega = (-1,1)^2 \setminus (0,1) \times (-1,0)$  and the exact solution is taken as

$$u(x,y) = r^{2/3}\sin(2\theta/3) + \exp(-(1000(x-0.5)^2 + 1000(y-0.5)^2)),$$
 (4.6)

which exhibits low regularity at the reentrant corner, located at the origin along with a sharp Gaussian at the point (0.5,0.5) (shown in Fig. 18) which initially is not resolved by the mesh. The same problem has been tested in reference [8].

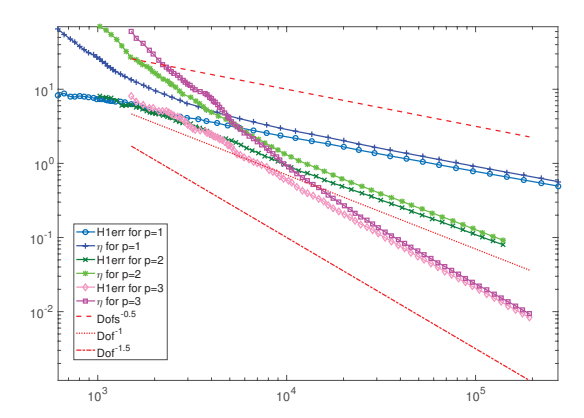


Figure 17: Example 4.6: Convergence results for initial polygonal mesh.

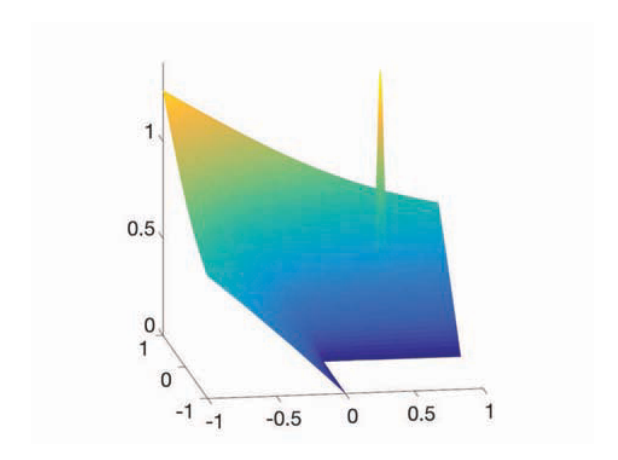


Figure 18: Example 4.7: Solution of the problem.

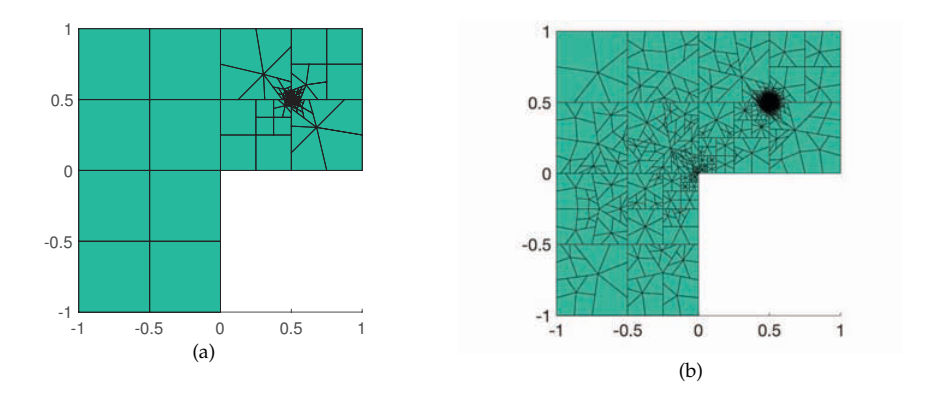


Figure 19: Example 4.7 for p=1: (a) mesh of 20 refinement; (b) mesh of 40 refinement.

In the adaptivity refinement with polynomial degree p=1, the first 20 refinement is to address the Gaussian peak centred at (0.5,0.5) (shown as Fig. 19 (a)). Once the Gaussian peak is sufficiently resolved, the refinement will be around the singularity at the reentrant corner. The adaptive mesh with level 40 is shown in Fig. 19 (b).

## Acknowledgments

This research was supported in part by the National Science Foundation Grants DMS-1418853 and DMS-1819041, by the Natural Science Foundation of China Grant 11628104, and by the Wayne State University Career Development Chair Grant.

The second author's research is based upon work supported in part by the U.S. Department of Energy, Office of Advanced Scientific Computing Research, Applied Mathematics program under award number ERKJE45; and by the Laboratory Directed Research and Development program at the Oak Ridge National Laboratory, which is operated by UT-Battelle, LLC., for the U.S. Department of Energy under Contract DE-AC05-00OR22725

This research was supported in part by National Science Foundation Grant DMS-1620016.

#### References

- [1] M. Ainsworth and J. Oden, A posteriori error estimation in finite element analysis, Pure Appl. Math., Wiley-Interscience, New York, 2000.
- [2] M. Ainsworth, A posteriori error estimation for discontinuous Galerkin finite element approximation, SIAM J. Numer. Anal.,45 (2007), 1777-1798.
- [3] I. Babuska and W. Rheinboldt, A-posteriori error estimates for the finite element method, Numer. Meth. in Eng., 12 (1978), 1597-1615.
- [4] R. Becker, P. Hansbo and M. Larson, Energy norm a posteriori error estimation for discontinuous Galerkin methods, Comput. Methods Appl. Mech. Engrg., 192 (2003), 723-733.
- [5] L. Beirao da Veiga, K. Lipnikov, and G. Manzini, Convergence analysis of the high-order mimetic finite difference method, Numer. Math., 113 (2009), 325-356.
- [6] L. Beirao da Veiga, F. Brezzi, A. Cangiani, G. Manzini, D. Marini and A. Russo, Basic principles of virtual element methods, Math. Models Methods Appl. Sci., 23 (2013).
- [7] Z. Cai, X. Ye and S. Zhang, Discontinuous Galerkin finite element methods for interface problems: a priori and a posteriori error estimations, SIAM J. Numer. Anal., 49 (2011), 1761-1787.
- [8] A. Cangiani, E. Georgoulis, T. Pryer and O. Sutton, A posteriori error estimates for the virtual element method, Numer. Math., 137 (2017): 857-893.
- [9] L. Chen, J. Wang and X. Ye, A posteriori error estimates for Weak Galerkin finite element methods for second order elliptic problem, J. of Sci. Comp., 59 (2014), 496-511.
- [10] B. Cockburn, J. Gopalakrishnan, and R. Lazarov, Unified hybridization of discontinuous Galerkin, mixed, and conforming Galerkin methods for second order elliptic problems, SIAM J. Numer. Anal., 47, (2009), 1319-136.

- [11] Z. Dong, E. Georgoulis and T. Pryer, Recovered finite element methods on polygonal and polyhedral meshes, arXiv:1804.08259.
- [12] R. Duran, Mixed Finite Element Methods. Class Notes (2007).
- [13] E. Georgoulis and T. Pryer, Recovered finite element methods, Comput. Methods Appl. Mech. Engrg., 332 (2018), 303-324.
- [14] P. Grisvard, Elliptic Problems in Nonsmooth Domains, SIAM, 2011.
- [15] P. Houston, D. Schtzau and T, Wihler, Energy norm a posteriori error estimation of hp-adaptive discontinuous Galerkin methods for elliptic problems, Math. Mod. Meth. Appl. Sci., 17 (2007), 33-62.
- [16] O. Karakashian and F. Pascal, A posteriori error estimates for a discontinuous Galerkinap-proximation of second order elliptic problems, SIAM J. Numer. Anal., 45 (2003), 1777-1798.
- [17] L. Mu, J. Wang and X. Ye, Weak Galerkin finite element method for second-order elliptic problems on polytopal meshes, Int. J. of Numer. Anal. and Model., 12 (2015), 31-53.
- [18] L. Mu, J. Wang, X. Ye and S. Zhang, A weak Galerkin finite element method for the Maxwell equations, J. of Sci. Comput., 65 (2015), 363-386.
- [19] L. Mu, J. Wang, X. Ye and S. Zhao, A new weak Galerkin finite element method for elliptic interface problems, J. Comput. Phy., 325 (2016), 157-173.
- [20] R. Nochetto, K. Siebert and A. Veeser, Theory of adaptive finite element methods: An introduction. In: DeVore R., Kunoth A. (eds) Multiscale, Nonlinear and Adaptive Approximation, Springer, Berlin, Heidelberg (2009).
- [21] D. Pietroa, E, Flauraudb, M. Vohralkc and S. Yousef, A posteriori error estimates, stopping criteria, and adaptivity for multiphase compositional Darcy flows in porous media, J. Comput. Phy., 276 (2014), 163-187.
- [22] D. Pietro and A. Ern, Hybrid high-order methods for variable-diffusion problems on general meshes, Comptes Rendus Mathmatique 353 (2015), 31-34.
- [23] C. Talischi, G. Paulino, A. Pereira and I. Menezes, PolyMesher: a general-purpose mesh generator for polygonal elements written in Matlab, Struct. Multidisc Optimiz., 45 (2012),309-328.
- [24] R. Verfurth, A review of a posteriori error estimation and adaptive mesh-refinement techniques, Teubner Skripten zur Numerik. B.G. Willey-Teubner, Stuttgart, 1996.
- [25] J. Wang and X. Ye, A Weak Galerkin mixed finite element method for second-order elliptic problems, Math. Comp., 83 (2014), 2101-2126.
- [26] R. Wang, X. Wang, and R. Zhang, A modified weak Galerkin finite element method for the poroelasticity problems, Numer. Math. Theor. Meth. Appl. 11 (2018): 518-539.
- [27] J. Wang and X. Ye, A weak Galerkin finite element method for the Stokes equations, Adv. in Comput. Math., 42 (2016), 155-174.
- [28] Q. Zhai, R. Zhang, N. Malluwawadu and S. Hussain, The weak Galerkin method for linear hyperbolic equation, Commun. Comput. Phys., 24 (2018): 152-166.
- [29] X. Zheng and X. Xie, A posteriori error estimation for a weak Galerkin finite element discretization of Stokes equations, East Asian Journal on Appl. Math., 7 (2017), 508-529.